

Graph Pattern Mining and Learning through User-defined Relations (Extended Version)

Carlos H. C. Teixeira*, Leonardo Cotta#, Bruno Ribeiro#, Wagner Meira Jr.*

*Department of Computer Science
Universidade Federal de Minas Gerais
Belo Horizonte, Brazil
{carlos,meira}@dcc.ufmg.br

#Department of Computer Science
Purdue University
West Lafayette, IN
{cotta,ribeirob}@purdue.edu

Abstract—In this work, we propose R-GPM, a parallel computing framework for graph pattern mining (GPM) through a user-defined subgraph relation. More specifically, we enable the computation of pattern statistics through their subgraph classes, generalizing traditional GPM methods. R-GPM provides efficient estimators for these statistics by employing an MCMC sampling algorithm combined with several optimizations. We provide both theoretical guarantees and empirical evaluations of our estimators in application scenarios such as stochastic optimization of higher-order graph neural network models and pattern (motif) counting. We also propose and evaluate optimizations that enable improvements of our estimators accuracy, while reducing their computational costs in up to 3-orders-of-magnitude. Finally, we show that R-GPM is scalable, providing near-linear speedups on 44 cores in all of our tests.

I. INTRODUCTION

Graph pattern mining (GPM) consists of finding *relevant* patterns in labeled graphs (networks¹). A pattern is a template of subgraphs, say, two females and two males in a social network connected as a fully connected 4-node subgraph. Further, the relevance of a pattern is given by the properties of its occurrences in the graph. For example, in frequent subgraph mining, a subgraph template is considered relevant if it occurs frequently in the network, i.e., the relevance criterion is based on the popularity of the graph patterns [1], [2].

In the last decades, a variety of GPM methods have emerged with the purpose to speedup existing algorithms [3], [4]. These techniques are used in several high-impact applications, such as label and link prediction [5] and the analysis of biological networks [6], semantic (RDF) graphs [7], citation and social networks [8], [9]. More recently, there has been growing interest in specific properties of these patterns [10], [11].

Despite the huge interest in GPM applications, existing methods are usually restricted to specific tasks. Moreover, designing an efficient algorithm for a given GPM task is usually hard, since even reasonably-sized real-world networks ($> 10k$ nodes) tend to have a massive number of k -node subgraphs ($k \geq 4$), which may let the mining process impracticable.

This work generalizes GPM tasks through user-defined local *subgraph relations*, and introduces an efficient sampling

algorithm to estimate user-defined subgraph statistics over the subgraph classes that arise from these relationship definitions. Let $\mathcal{S}^{(k)}$ be the set of all k -node induced subgraphs of G . A subgraph relation R splits $\mathcal{S}^{(k)}$ into partitions or *subgraph classes*, where a pair of subgraphs $S, S' \in \mathcal{S}^{(k)}$ belongs to the same *subgraph class* iff they have relationship R . Our task is to compute the relevance of a pattern as a function of its subgraph classes in G .

From the practitioner’s point of view, relations provide strong advantages over traditional methods: (a) a novel pattern analysis task is defined by simply setting a new subgraph relation; (b) relations are flexible and several subgraph relations may be developed by a user. For instance, a relation may consider the spatial location of the subgraphs, the attributes of their nodes and edges, or even complex networks metrics (e.g., centrality, clustering coefficient, etc); (c) subgraph relations organize $\mathcal{S}^{(k)}$ into partitions, which may be used to understand and interpret the relevant patterns reported by the algorithm. Finally, (d) they generalize the existing GPM solutions since each subgraph can be considered as a class itself, i.e., $SR S'$ is true iff $S = S'$.

To the best of our knowledge, there is no efficient algorithms able to compute statistics of patterns based on user-defined subgraph relations. A naïve method would have to (1) enumerate the subgraph set $\mathcal{S}^{(k)}$ and, (2) doubly-iterate over $\mathcal{S}^{(k)}$ testing $SR S'$ for all pairs of $S, S' \in \mathcal{S}^{(k)}$, which is computationally intractable even in moderate-sized graphs.

Contributions: This paper introduces a generalized GPM task and an efficient and parallel sampling framework, R-GPM, to estimate relevance criteria for a large family of user-defined relations and summarization functions. Our method computes statistics of the subgraph classes by integrating a computationally bounded exact algorithm with an unbiased estimator based on random walks, through a novel use of the renewal-reward theorem of Markov chains. More specifically, R-GPM is able to take advantage of an incomplete subgraph class’ computation to improve the estimator accuracy in two complementary ways: (a) by only estimating the residual that has not been computed exactly, and (b) by parallelizing and reducing the variance associated with random walk sampling using the subgraphs of the exact computation as a stopping

¹Throughout this work we will use the terms *graph* and *network* interchangeably.

set for the random walk.

We also introduce a host of innovations in random walk sampling for subgraph relevance score estimation, such as non-backtracking random walks, data structure optimizations and parallel unbiased estimators using random walks. In particular, R-GPM adopts a *producer-consumer* parallelization model which provides a near-linear speedup on 44 cores. Moreover, we show that subgraph relations can be useful in tasks ranging from a Robbins-Monro [12] stochastic optimization method to train deep neural networks for subgraph evolution prediction, to a generalization of k -clique percolation using any k -connected subgraph [13].

Reproducibility: Our open-sourced code and the data we used are at <http://github.com/dccspeed/rgpm>.

II. PRELIMINARIES

GPM problems take an attributed undirected graph $G = (V, E, \Phi)$, where V (also denoted as $V(G)$) is defined as the set of vertices, E is the set of edges ($E(G)$) and $\Phi(v, G)$ is the label of node $v \in V$ in G .

Let S be a *connected and induced subgraph* (CIS) in G . S is induced if it has a set of nodes $V(S) \subset V(G)$ and a set of edges $E(S)$ containing all edges in $E(G)$ that have both endpoints in $V(S)$. In addition, S is connected when there is a path between any pair of nodes in $V(S)$ formed by the edges in $E(S)$. The subgraphs used in this work are all CISes.

Roughly speaking, a pattern is a graph template. We define a pattern (or canonical representation) of a subgraph S , $\rho(S)$, as its canonical labelling code [14]. Therefore, if two subgraphs S and S' are *isomorphic*, then, $\rho(S) = \rho(S')$. Note that our approach is not tied to this labelling and other representation form can be used (e.g. [15], [16]).

Problem statement: Given a user-defined relation R , computing the pattern relevance score demands the instantiation of three functions: (i) g , the subgraph function; (ii) α , the class weight function; and (iii) F , the pattern statistic function. g is an arbitrary user-defined function ($|g(\cdot)| < \infty$) and, intuitively, it quantifies the contribution of a subgraph to its pattern's score. As we will see, g is the basis of both α and F functions.

The first part of our problem is to compute the *class weight function*, $\alpha(\cdot)$, for the class of given subgraph S , iterating over all CISes in $\mathcal{S}^{(k)}$ as follow:

$$\alpha(R, S) = \sum_{S' \in \mathcal{S}^{(k)}} g(S') \cdot \mathbf{1}_{\{S'RS\}}, \quad (1)$$

where $\mathbf{1}_{\{S'RS\}} = 1$ iff subgraphs $S', S \in \mathcal{S}^{(k)}$ have relationship R , otherwise $\mathbf{1}_{\{S'RS\}} = 0$.

Finally, the last part of our problem is to compute the relevance score of a pattern P in a graph G . This is given by the *pattern statistic function*, F , which is given by:

$$F(G, R, P) = \frac{1}{\lambda} \sum_{S \in \mathcal{S}^{(k)}} \frac{\alpha(R, S)}{|C_{R,S}|} \cdot \mathbf{1}_{\{\rho(S)=P\}}, \quad (2)$$

where $\rho(S)$ is a function that gives the pattern of subgraph S , $C_{R,S}$ is the set of subgraphs related to S or, formally, $C_{R,S} = \{S' \in \mathcal{S}^{(k)} | \mathbf{1}_{\{S'RS\}} = 1\}$ and λ is the normalization

factor equal to $\sum_{S \in \mathcal{S}^{(k)}} \frac{\alpha(R, S)}{|C_{R,S}|}$. Trivially, if $g(S) = \frac{1}{|C_{R,S}|}$, F returns the proportion of classes that a pattern P has in G , while the standard motifs counting problem arises for $g(\cdot) = 1$ and $\mathbf{1}_{\{S'RS\}} = 1$ iff $S' = S$.

Note that, computing both α and F are computationally expensive since they require a sum over all CISes in $\mathcal{S}^{(k)}$. Our framework overcomes this issue by estimating α and F through MCMC sampling (as shown in Section III).

Equivalence-isomorphic relation R . Despite the variety of possible relations R , this work focuses on a special group, which we denote *equivalence-isomorphic* relations.

Definition 1 (Equivalence-isomorphic relation). *We define an equivalence-isomorphic relation R as satisfying the following properties: (1) reflexivity: a relation R is reflexive if for all $S \in \mathcal{S}^{(k)}$, $SR S$; (2) symmetry: a relation R is symmetric if for all $S, S' \in \mathcal{S}^{(k)}$, $SR S'$ implies $S'RS$; (3) transitivity: a relation R is transitivity if for all $S, S', S'' \in \mathcal{S}^{(k)}$, $SR S'$ and $S'RS''$ implies $SR S''$; (4) isomorphic: a relation R is isomorphic if for all $S, S' \in \mathcal{S}^{(k)}$, $SR S'$ implies that S and S' are attributed-isomorphic (i.e., $\rho(S) = \rho(S')$).*

Equivalence-isomorphic relations have the advantage of producing homogeneous classes w.r.t. patterns, where a class can be directly assigned to its pattern. We study two instances of these relations in our experiments: (1) pattern percolation and (2) shared hubs (defined in Section IV).

III. RELATION-BASED GRAPH PATTERN MINING

This section presents our framework R-GPM to compute and estimate α and F for all subgraphs and patterns in the input graph G . The central idea of R-GPM is to reduce the number of relation tests ($SR S'$) by employing sampling methods on a high-order network (HON) of G .

The HON used in our framework, also denoted by $G^{(k)}$, has its nodes composed by k -node CISes in G , where two CISes have an edge if they share $k-1$ nodes (Def. 2). R-GPM builds $G^{(k)}$ on the fly for subgraph sampling using MCMC output sampling [17], [18], [19]. This MCMC process is performed through a *random walk* (RW) over $G^{(k)}$, keeping in memory only a single k -HON neighborhood at a time (Def. 3).

Definition 2 (k -HON of G , or $G^{(k)}$). *A k -HON $G^{(k)} = (\mathcal{S}^{(k)}, E^{(k)})$ is a network where $\mathcal{S}^{(k)}$ composes the set of nodes and $E^{(k)}$ represents the set of edges in $G^{(k)}$. More specifically, $E^{(k)} = \{(S, S') | S \in \mathcal{S}^{(k)}, S' \in \mathcal{S}^{(k)} \text{ and } |V(S) \cap V(S')| = k-1\}$.*

Definition 3 (k -HON Neighborhood, $N^{(k)}(S)$). *The k -HON neighborhood of a k -node subgraph S in $G^{(k)}$ or, simply, $N^{(k)}(S)$, is composed by subgraphs that share $k-1$ nodes with S . Formally, $N^{(k)}(S) = \{S' | S' \in \mathcal{S}^{(k)} \text{ and } |V(S) \cap V(S')| = k-1\}$.*

However, existing CIS sampling methods **cannot** estimate both F and α (eqs. (1) and (2)) since the asymptotic convergence of the estimate F requires an exact computation of α . Moreover, for some subgraph classes, an exact computation

of α may be faster than MCMC sampling. R-GPM combines an sampling technique with an exact computation algorithm achieving benefits from both.

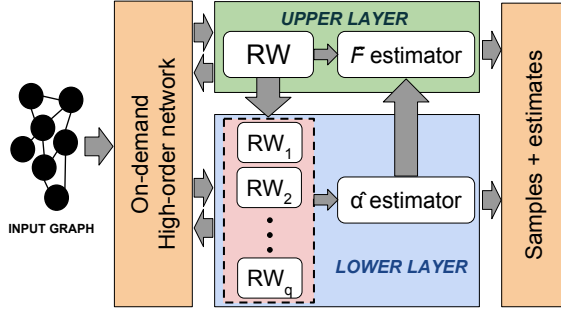


Fig. 1: R-GPM framework has two computation layers, the upper and the lower. They estimate α and F (eqs. (1) and (2)) in parallel, following a producer-consumer model.

Framework overview. Our parallel computing framework R-GPM has two computation layers, denoted upper and lower. The *upper layer* is responsible for estimating F , while the *lower* one estimates α . As shown in Figure 1, R-GPM receives a input graph and builds on-demand (i.e., when requested by a layer) the HON $G^{(k)}$. The upper layer performs a RW on $G^{(k)}$ to sample subgraphs whose classes (and their α 's) will be computed.

Let S be a subgraph sampled in the upper layer. Then, S is sent to the lower layer, which produces a *finite-sample unbiased* estimate of $\alpha(R, S)$ (eq. (1)) from q independent random walks processes on $G^{(k)}$ (depicted in Fig. 1 by the dotted lined block). The estimated value of α is returned to the upper layer in order to compute F (eq. (2)), with a consistent estimator. At the end, the subgraphs sampled by R-GPM and the all estimates of α and F are given to the user.

R-GPM parallelizes the tasks from the two computation layers following a *producer-consumer* model. This model fits naturally in our mining process since the producer and consumer roles can be mapped directly to the upper and lower layers, respectively. In addition, as the RWs procedures in the lower layer are independent, they are also computed simultaneously by R-GPM.

A. Computing α (lower layer)

In the lower layer, R-GPM receives a subgraph and it runs an exact computation of α , limited to a computational budget B w.r.t. the number of subgraphs that our framework can generate. Once budget B is exhausted, R-GPM switches to a sampling procedure for estimating α . One of our main contributions is an unbiased estimator of α that leverages the output of the exact computation algorithm in order to improve our estimator in terms of both accuracy and efficiency.

1) *Iteration-bounded exact computation:* The iteration-bounded exact method is detailed in Algorithm 1, where we traverse $G^{(k)}$ with a BSF algorithm. Starting from a subgraph S , given as parameter, our exact method iterates (or visit)

Algorithm 1: Iteration-bounded Class Computation

input : G , a input graph
input : S , a k -node subgraph
input : R , a user-defined subgraph relation
input : B , the maximum number of steps allowed
input : $g(\cdot)$, a user-defined function to compute $\alpha(C)$
input : $h(\cdot)$, a user-defined function to restrict $G^{(k)}$ (optional)
output : α , the weight value of S 's class
output : $C_{R,S}$, the class of S with relation R
output : c , a boolean to say if $C_{R,S}$ is complete.

```

1  $\alpha \leftarrow 0$ ;
2  $C_{R,S} \leftarrow \emptyset$ ;
3  $H \leftarrow \{S\}$ ;
4  $Q.push(S)$ ; // queue of subgraphs
   /* Verify all non-visited subgraphs. */
5 while  $Q \neq \emptyset$  do
6    $S' \leftarrow Q.pop()$ ;
7   for  $S'' \in N^{(k)}(S') \setminus H$  do
8     /* Verify if  $S''$  must be visited. */
9     if  $h(S'') = \text{true}$  then
10       $H \leftarrow H \cup \{S''\}$ ;
11       $Q.push(S'')$ ;
12      /* Update values if related. */
13      if  $S''R = \text{true}$  then
14         $\alpha \leftarrow \alpha + g(S'')$ ;
15         $C_{R,S} \leftarrow C_{R,S} \cup \{S''\}$ ;
16      if  $|H| = B$  then
17        return  $\alpha, C_{R,S}, \text{false}$ ;
18 return  $\alpha, C_{R,S}, \text{true}$ 

```

on up to B CISEs. Foremost, it starts by setting α , $C_{R,S}$, H and Q to their initial values (lines 1-4). While there are subgraphs to be visited in the queue Q , we search for unvisited subgraphs (lines 7-15). If the subgraph under analysis (S'') is valid according $h(\cdot)$, we add it in the set of visited subgraphs H and in queue Q for further inspection (lines 9-10). Note that $h(\cdot)$ is an optional function that one may define in order to prune the search space and, if $h(\cdot)$ is not given, all subgraphs are valid by default. The ideal (faster) scenario emerges when $h(\cdot)$ restricts the subgraph exploration to only subgraphs in $C_{R,S}$. Moreover, α and $C_{R,S}$ are updated if S'' is R-related to subgraph S (12-13). The algorithm returns in two cases: (1) if the budget for traversing $G^{(k)}$ is finished and $C_{R,S}$ is incomplete (lines 14-15) or (2) when there is no unchecked subgraph in Q and $C_{R,S}$ was completely generated (line 16).

In worst case, the time complexity of Algorithm 1 is $O(\min(B, |S^{(k)}|)^2)$ when $G^{(k)}$ is dense. In addition, the amount of memory necessary to run the exact method is bounded by $O(\min(B, |S^{(k)}|) + |V(G)|)$, where $|V(G)|$ is the space required to keep $N^{(k)}(S)$ of a certain subgraph S for small values of k ($k < 10$).

2) *Estimating α via sampling:* We propose to estimate $\alpha(R, S)$ by performing *random walk tours* (RWTs) on $G^{(k)}$. A RWT on G is a special type of random walk that considers the first-return time of the RW Markov chain (i.e., the first time the RW returns to the starting node) to estimate network statistics from sampled nodes [20], [21]. To the best of our

knowledge, this is the first work that applies RWTs on high-order networks which is particularly challenge due to the large number of nodes in $G^{(k)}$ (k -node subgraphs). Next, we introduce a variety of innovations and optimizations to deal with this issue.

- *Reusing the exact computation to speed-up return times:* The return time (steps) of a RW to the same initial state can already be prohibitively on $G^{(k)}$. To speed-up return times, we transform the subgraphs retrieved in an iteration-bounded exact computation of α , specifically the ones that belong to the class $C_{R,S}$, in a collapsed supernode. The supernode is a *virtual* node of $G^{(k)}$ with a massive number of edges, which speeds-up return times, as the expected return time is inversely proportional to the number of edges of a node [21]. We call this collapsed node a supernode and denote it \mathcal{I}_S , and it often refers to it as both as a set and as a *collapsed node*.
- *Non-backtracking random walks:* On the other hand, very short return times can point to a poor mixing of the random walk, where the massive degree of supernode \mathcal{I}_S impedes the exploration of $G^{(k)}$ by the walkers. To overcome this challenge, we use *non-backtracking random walks* (nRWs). The advantage of nRWs over the ordinary RWs is that it avoids resampling recently sampled nodes [22], [23], ensuring return times greater than two. We denote this approach a *non-backtracking random walk tour* (nRWT).

The $\hat{\alpha}$ estimator: Theorem 1 shows an unbiased estimator of α using nRWTs.

Theorem 1. *Let G be the input graph, R be a user-defined relation and $g(\cdot)$ a user-defined function. Moreover, consider S a subgraph in $\mathcal{S}^{(k)}$, \mathcal{I}_S (supernode) a set of subgraphs related to S and $\mathcal{T}^r = \{S_1^r, \dots, S_T^r\}$ the sample path of subgraphs visited by the r -th RWT on $G^{(k)}$, where $1 < r < q$ and S_i^r is the subgraph reached by the RWT in step i . Because \mathcal{T} is a RWT, $S_1 \subseteq \mathcal{I}_S$, $S_T \subseteq \mathcal{I}_S$ and $S_j \not\subseteq \mathcal{I}_S$, $\forall 1 < j < T$. Then*

$$\hat{\alpha}(q, R, S) = \frac{\sum_{S' \in \mathcal{I}_S} |N^{(k)}(S') \setminus \mathcal{I}_S|}{q} \sum_{r=1}^q \sum_{i=2}^{|\mathcal{T}^r|-1} \frac{g(S_i^r) \cdot \mathbf{1}_{\{S_i^r \subseteq \mathcal{I}_S\}}}{|N^{(k)}(S_i^r)|} \quad (3)$$

$$+ \sum_{S' \in \mathcal{I}_S} g(S') \cdot \mathbf{1}_{\{S' \subseteq \mathcal{I}_S\}}$$

is an unbiased estimator of $\alpha(R, S)$.

The proof of Theorem 1 is broken down into multiple parts. First, we formalize the non-backtracking RW on $G^{(k)}$, and show its steady state is the same as the steady state of a standard RW.

Definition 4 (nRW on $G^{(k)}$). *A nRW on $G^{(k)}$ is a 2nd order Markov chain with transition probability matrix:*

$$\mathbf{T}(S|S', S'') = \begin{cases} 0 & , \text{ if } S = S'', |N^{(k)}(S')| > 1 \\ 1 & , \text{ if } S = S'', |N^{(k)}(S')| = 1 \\ \frac{1}{|N^{(k)}(S')|-1} & , \text{ otherwise,} \end{cases} \quad (4)$$

where S, S', S'' are k -node CISEs in $\mathcal{S}^{(k)}$.

Lemma 1. *The steady state distribution π of the nRW 2nd order Markov chain given by the transition probability matrix \mathbf{T} of Definition 4 is:*

$$\pi(S) = \frac{|N^{(k)}(S)|}{\sum_{S' \in \mathcal{S}^{(k)}} |N^{(k)}(S')|}, \quad (5)$$

where $|N^{(k)}(S)|$ is the number of neighbors of S in the k -HON $G^{(k)}$, as described in Definition 3.

The proof of Lemma 1 comes from the fact that the resulting 2nd order Markov chain is irreducible, aperiodic, and Harris recurrent [24], as long as a random walk on $G^{(k)}$ provides such properties. As $G^{(k)}$ is finite, the chain is trivially Harris recurrent. Moreover, a Markov chain on $G^{(k)}$ is irreducible and aperiodic since $G^{(k)}$ is a strongly connected and non-bipartite graph [25], which is shown next.

Lemma 2. *$G^{(k)}$ is a strongly connected and non-bipartite graph $\forall k \in \{i|2 \leq i \leq m-1\}$ if (a) G is a strongly connected component and (b) G has a cycle with m nodes and m is odd.*

Proof. Let $L = \{v_1, \dots, v_m\}$ be the set of nodes that composes a cycle in a strongly connected graph G , where $|L| = m$, v_1 is connected to v_m , v_i is connected to v_{i+1} and m is a odd number. As L is connected by definition, we may enumerate CISEs from their nodes. Let $L^{(k)}$ be the set of k -node subgraphs using *only* the nodes in L . Then, $L^{(k)}$ has exactly m CISEs, $\forall k \in \{i|2 \leq i \leq m-1\}$.

We now need to show that these m k -node subgraphs generate a cycle in $G^{(k)}$. Let $L^{(k)} = \{S_1, \dots, S_m\}$ where $V(S_i) = \{v_i, \dots, v_w\}$ and $w = i + k - 1 \bmod m$. For instance, considering $k = 2$ and $m = 3$, we have $V(S_1) = \{v_1, v_2\}$ and $V(S_3) = \{v_3, v_1\}$. These k -node subgraphs are connected in $G^{(k)}$ whenever they share $k - 1$ nodes between them, according to Definition 2, i.e., S_i is connected to S_{i-1} and S_{i+1} in $G^{(k)}$, $\forall i \in \{2 \leq i \leq m-1\}$. \square

Now that we know how nRWs have the same steady state distribution as RWs, the proof concludes with Lemma 3, showing that we can construct an unbiased estimator of α from the sample path of each nRWT.

Lemma 3. *Let \mathcal{T}^r be the set of sampled nodes in the r^{th} nRWT on $G^{(k)}$, $r \geq 1$ starting at the supernode \mathcal{I}_S . Then,*

$$\mathbb{E} \left[\sum_{S' \in \mathcal{I}_S} |N^{(k)}(S') \setminus \mathcal{I}_S| \sum_{i=2}^{|\mathcal{T}^r|-1} \frac{g(S_i^r) \cdot \mathbf{1}_{\{S_i^r \subseteq \mathcal{I}_S\}}}{|N^{(k)}(S_i^r)|} + \sum_{S' \in \mathcal{I}_S} g(S') \cdot \mathbf{1}_{\{S' \subseteq \mathcal{I}_S\}} \right] = \alpha(R, \mathcal{I}_S) \quad (6)$$

Proof. We start by rewriting Eq. 6 as

$$|N^{(k)}(S') \setminus \mathcal{I}_S| \mathbb{E} \left[\sum_{S' \in \mathcal{I}_S} \sum_{i=2}^{|\mathcal{T}^r|-1} \frac{g(S_i^r) \cdot \mathbf{1}_{\{S_i^r \subseteq \mathcal{I}_S\}}}{|N^{(k)}(S_i^r)|} \right] = \alpha(R, \mathcal{I}_S) - \sum_{S' \in \mathcal{I}_S} g(S') \cdot \mathbf{1}_{\{S' \subseteq \mathcal{I}_S\}} \quad (7)$$

With the nRW starting at \mathcal{I}_S , we can rewrite the expected value on the left hand side of eq. (7) as

$$\mathbb{E}\left[\sum_{i=2}^{|\mathcal{T}^r|-1} \frac{g(S_i^r) \cdot \mathbf{1}_{\{S_i^r \in \mathcal{R}_S\}}}{|N^{(k)}(S_i^r)|}\right] = \sum_{S^{(k)} \in \mathcal{I}_S} \mathbb{E}\left[\frac{\mathbb{S}_i^r g(S_i^r) \cdot \mathbf{1}_{\{S_i^r \in \mathcal{R}_S\}}}{|N^{(k)}(S_i^r)|}\right], \quad (8)$$

where \mathbb{S}_i^r is the number of times the Markov Chain reaches S_i in the r^{th} tour.

Given a renewal-reward process with inter-reward time distributed as $|\mathcal{T}^r|$, $r \geq 1$ and reward \mathbb{S}_i^r , the renewal theorem gives us that

$$\pi(S_i^r) = \mathbb{E}[|\mathcal{T}^r|]^{-1} \mathbb{E}[\mathbb{S}_i^r].$$

Hence, 8 becomes

$$\begin{aligned} \sum_{i=2}^{|\mathcal{T}^r|-1} \mathbb{E}\left[\frac{\mathbb{S}_i^r g(S_i^r) \cdot \mathbf{1}_{\{S_i^r \in \mathcal{R}_S\}}}{|N^{(k)}(S_i^r)|}\right] &= \\ \sum_{i=2}^{|\mathcal{T}^r|-1} \frac{\mathbb{E}[|\mathcal{T}^r|] \pi(S_i^r) g(S_i^r) \cdot \mathbf{1}_{\{S_i^r \in \mathcal{R}_S\}}}{|N^{(k)}(S_i^r)|} \end{aligned} \quad (9)$$

Moreover, it follows from Kac's theorem that $\mathbb{E}[|\mathcal{T}^r|] = \frac{1}{\pi(\mathcal{I}_S)}$. Thus, by leveraging Lemma 1 we can rewrite eq. (9) now as

$$\begin{aligned} \sum_{i=2}^{|\mathcal{T}^r|-1} \frac{\mathbb{E}[|\mathcal{T}^r|] \pi(S_i^r) g(S_i^r) \cdot \mathbf{1}_{\{S_i^r \in \mathcal{R}_S\}}}{|N^{(k)}(S_i^r)|} &= \\ = \frac{1}{\sum_{S' \in \mathcal{I}_S} |N^{(k)}(S')|} \sum_{i=2}^{|\mathcal{T}^r|-1} g(S_i^r) \cdot \mathbf{1}, \end{aligned} \quad (10)$$

and see that since the tours only compute the function outside the supernode, Lemma (3) follows directly from eq. (8) as we wanted to show. \square

Proof of Theorem 1. By the Strong Markov Property, each tour is independent of the others. Thus, by Lemma 3 and linearity of expectation, Theorem 1 holds. \square

B. Estimating F (upper layer)

The ordinary RW on $G^{(k)}$ can be seen as sampling of subgraph classes, where the class $C_{R,S}$ is sampled whenever S is visited by the MCMC process, for any relation R of interest. Thus, we may estimate F (eq. (2)) using a simple RW on $G^{(k)}$, with asymptotic bias given by the number of CISes in the classes. Fortunately, such bias may be removed using the Horvitz-Thompson estimator [26]. Theorem 2 gives a consistent estimator of F of eq. (2).

Theorem 2. Let $\mathcal{M}_t = \{S_1, \dots, S_t\}$ be CISes visited by the upper layer RW over $G^{(k)}$ after $t > 1$ steps. Consider the estimator

$$\hat{F}(t, q, G, R, P) = \frac{1}{\lambda} \sum_{S \in \mathcal{M}_t} \frac{\hat{\alpha}_1(q, R, S) \cdot \mathbf{1}_{\{P(S)=P\}}}{\hat{\alpha}_2(q, R, S)}, \quad (11)$$

where $\hat{\alpha}_1$ estimates $\alpha(R, S)$, and $\hat{\alpha}_2$ estimates $\sum_{S' \in C_{R,S}} |N^{(k)}(S')|$ (the steady state probability a CIS in $C_{R,S}$ is sampled by the upper layer random walk), $q \propto t$ is the number of tours used in the estimates of $\hat{\alpha}_1$ and $\hat{\alpha}_2$, and $\lambda = \sum_{S \in \mathcal{M}_t} \frac{\hat{\alpha}_1(q, R, S)}{\hat{\alpha}_2(q, R, S)}$. Then, \hat{F} is consistent (asymptotically unbiased), that is,

$$\lim_{t \rightarrow \infty} \hat{F}(t, q, G, R, P) \stackrel{a.s.}{=} F(G, R, P).$$

Proof (sketch). The main challenge is to prove that the ratio $\hat{\alpha}_1/\hat{\alpha}_2$ in eq. (11) does not create issues in the asymptotic

convergence. From Lemma 3 we know that $\hat{\alpha}_1$ and $\hat{\alpha}_2$ are both unbiased and i.i.d. for any number of tours q . And we can make an infinite number of tours $q \propto t \rightarrow \infty$ because tours are finite a.s. [21]. Averaging $\hat{\alpha}_1$ and $\hat{\alpha}_2$ over all such tours gives a.s. convergence by the Strong Law of Large Numbers (SLLN). This means that we can directly use the SLLN for Markov chains [25] to establish a.s. convergence over the entire estimator. \square

IV. EXPERIMENTAL EVALUATION

In this section we evaluate the proposed method with real-world networks in two different tasks. First, we showcase two applications of our approach. Second, we empirically validate the accuracy of our estimator.

Hardware. We evaluate R-GPM in the XSEDE Jetstream [27] servers with Intel Xeon E5-2670 CPUs with a total of 44 execution threads at 2.5GHz per core and 120GB RAM.

Datasets. We used the following datasets in our evaluation.

Yeast: the Yeast protein-protein interaction dataset [28] is a graph, where proteins are nodes, an edge means an interaction and a node attribute gives the protein function. The largest component was considered and self loops were excluded, totaling 2224 nodes, 6609 edges and 13 labels.

DBLP- n : DBLP [29] is a bibliographic temporal network with three node types (authors, venues, and topics) which are connected by the publication of a paper. We define DBLP- n , as the DBLP snapshot given by publications between the years $[2001 + 2n, 2001 + 2n + 1]$, for $n = 1, 2, 3$. There are 22412 authors in all 3 networks, with up to 127851 edges.

Microsoft scientific research (MSR): This is a bibliometric network from the Microsoft scientific research dataset [30]. It contains authors and their collaborations considering only the data mining community². The largest connected component has 26855 nodes and 101320 edges. We considered the year of her first publication to determine the node attribute: (1) junior, (2) intermediate and (3) senior researcher.

Note that, although the input graphs have a relatively small number of nodes (up to 27k), their HONs are huge with up to 66M of nodes (subgraphs).

Subgraph relations. Our experiments consider two subgraph relations. The first subgraph relation, PERC (Definition 5), generalizes the k -clique percolation method [13]. Here, a subgraph class arises from percolating a specific subgraph pattern over the graph. Note that our definition uses a general pattern P , i.e., it is not restricted to cliques. However, sparse patterns should be avoided, specially in non-labeled graphs, since they may percolate across the whole network, losing meaning.

The second relation is *shared d -hubs* (SH_d) (Definition 6), where related subgraphs must also share the nodes whose degrees are larger than a specified threshold d . In fact, SH_d is particularly interesting when applied on scale-free networks since it may be used to reduce the bias induced by high-degree nodes in GPM methods.

²ICDE, ICDM, KDD, PAKDD, PKDD, RECSYS, SDM, TKDD, TKDE, VLDB and WSDM.

Definition 5 (Pattern Percolation, PERC). A subgraph S is related to (or percolates) S' iff: (a) $S = S'$ or (b) $|V(S) \cap V(S')| = k - 1$ and $\rho(S) = \rho(S')$ or (c) S percolates S'' and S' percolates S'' .

Definition 6 (Shared d -Hubs, SH_d). Let $N(v_i)$ be the set of neighbors of the node v_i in the input graph G and $H(S) = \{v_i \in V(S) \mid |N(v_i)| \geq d\}$ be the set of high degree nodes (hubs) of a subgraph S given a threshold d . Then, two subgraphs S, S' are related (or equivalent) iff: (a) $S = S'$ or (b) $H(S) = H(S')$ and $\rho(S) = \rho(S')$.

A. Application: motif class counting

Motif class counting (MCC) is a generalization of the standard motif counting (SMC) problem [31], where the frequency of a pattern P is given by the number of subgraph classes a pattern P has in the input graph G rather than the total number of matchings of p in G . The rationale behind MCC is that subgraphs belonging to a same class are equivalent and, then, they should not be counted twice. The SMC problem can be easily mapped to MCC by setting $1_{\{SRS'\}} = 1$ iff $S = S'$ and $g(\cdot) = 1$.

We apply MCC with PERC relation on the Yeast graph, where the relevance score of a pattern is measured by the proportion of classes it has in G , obtained from F (eq. (2)) with $g(S) = \frac{1}{C_{R,S}}$ in eq. (1). We consider only 4-node subgraphs which are quasi-cliques [32] with density greater than 0.5, i.e., each node is connected to at least other 2 nodes in the subgraph.

In this experiment, we consider 4-node subgraphs in quasi-cliques [32] with density is greater than 0.5, i.e., each node is connected to at least other 2 nodes.

To show that the frequent patterns in MCC are different from SMC, we compare the topology of the top frequent motifs obtained by the exact method and MCC in the Yeast graph. More specifically, we compute the Kendall's Tau correlation between two motifs' rankings: one returned by the exact and traditional method and the second ranking from MCC-PERC (converged). The result is given in Table I, where in consider different ranking' sizes. Indeed, we can't reject the hypothesis of the rankings being independent, showing empirically the difference between them.

Ranking Size	Test statistic	p-value
50	0.01	0.90
100	0.00	0.95
500	0.04	0.17

TABLE I: Comparison between two rankings of patterns returned by SMC and MCC-PERC in Yeast graph through Kendall Tau correlation. We reject the hypothesis of the rankings being independent as we increase the ranking' size.

A closer look also reveals fundamental structural differences between the SMC method and MCC. Table II shows topologies – colors represent protein functions – and relative frequencies (F) of the top 3 motifs listed by the two approaches evaluated.

Note that the patterns found by MCC are structurally different, having a greater diversity of protein functions (node attributes).


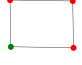

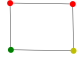
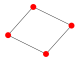
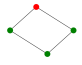
Rank	SMC	MCC-PERC
	F Motif	\hat{F} Motif
1	4.15 	0.58 
2	3.66 	0.56 
3	2.02 	0.41 

TABLE II: Comparison between the top 3 most frequent motifs obtained using SMC and MCC-PERC methods in Yeast graph. Indeed, the methods can find different relevant patterns.

B. Application: Subgraph Prediction

We now focus on the flexibility of our generalization of GPM by using it to train a deep neural network model that predicts subgraph dynamics on temporal graphs. For this task, we use the Subgraph Pattern Neural Network (SPNN) model of Meng et al. [5]. Consider a temporal graph $(G_n)_{n=1}^3$. Meng et al. predicts how CISEs (connected induced subgraphs) on G_1 will evolve in G_2 . More precisely, the goal of the model is to minimize the negative log-likelihood loss

$$\mathcal{L}(G_1; \mathbf{W}) = - \sum_{C \in \mathcal{S}_1^{(k)}} \log \Pr(y(S)|S, \mathbf{W}), \quad (12)$$

where \mathbf{W} are the neural network parameters, $\mathcal{S}_1^{(k)}$ are the k -node CISEs of G_1 and $y(S)$ is a class label indicating which subgraph S has evolved into on G_2 . For instance, for $k = 3$, S is a triangle or a vee on G_1 and $y(S) \in \{0, 1\}$ indicates whether S becomes disconnected or not on G_2 . Once \mathbf{W} learned by minimizing eq. (12), the model is applied to subgraphs on G_2 , predicting their evolution (labels) on G_3 . To scalably optimize eq. (12), we need to train the model with stochastic gradient descent, which samples CISEs on G_1 .

Considering that the degree distribution of real networks often follows a power law, we soon realize that the high-degree hubs on G_1 induce a large number of CISEs, which will have a disproportional influence over the objective function in eq. (12). Using R-GPM, practitioners now can reduce this influence by defining a subgraph relation in an alternative loss function to eq. (12):

$$\mathcal{L}'(G_1; \mathbf{W}) = - \sum_{S \in \mathcal{S}_1^{(k)}} \alpha(R, S) \log \Pr(y(S)|S, \mathbf{W}), \quad (13)$$

where $\alpha(R, S)$ is a weight of CIS S defined by relation R . Using R-GPM, we can efficiently estimate the required gradients of eq. (13), $\sum_{S \in \mathcal{S}_1^{(k)}} \alpha(R, S) \nabla_{\mathbf{W}} \log \Pr(y(S)|S, \mathbf{W})$, since our approach samples S from $\mathcal{S}_1^{(k)}$ with an asymptotically known bias and $\alpha(R, S)$ is estimated with a finite-sample

unbiased estimator. The result is asymptotically unbiased estimates of the gradient that we use in what is known as the Markovian dynamic case of the Robbins-Monro stochastic optimization [33].

Experiment: We consider the same task defined in Meng et al. for the DBLP dataset. Given an author, a venue and a topic, we want to predict whether the author will publish in this venue and in this topic in the next timestep. We consider DBLP as a sequence of 3 graphs (with a span of two years each). The subgraph relation R is SH_{100} . We use 6000 samples for training (evolution from G_1 to G_2) and 2500 for testing (evolution from G_2 to G_3). We use the same hyperparameters as in Meng et al.: 30% of our training data to perform early stopping, the maximum number of epochs is 6000, learning rate is set to 0.01, and L2 regularization strength is 0.001.

Results: To evaluate the training of SPNN with the estimated class weights $\hat{\alpha}$ in eq. (13), in the test phase, i.e., predicting how CISes in G_2 evolve on G_3 , we compute the weighted accuracy

$$W_{Acc} = \frac{\sum_{S \in \mathcal{S}_2^{(k)}} \alpha(R, S) \mathbf{1}_{\{\hat{y}(S; \mathbf{W}) = y(S)\}}}{\sum_{S \in \mathcal{S}_2^{(k)}} \alpha(R, S)},$$

where $\hat{y}(S; \mathbf{W})$ is the predicted evolution given by the trained model, $\mathcal{S}_2^{(k)}$ are the k -node CISes of G_2 . As $\alpha(R, S)$ is expensive to compute, we estimate W_{Acc} we use the approximation $\alpha(R, S) \approx \hat{\alpha}(100, R, S)$.

We used R-GPM to train the model against assuming all CISes have the same weight, i.e., $\alpha(R, S) = 1, \forall S \in \mathcal{S}_1^{(k)}$, i.e., we are biasing against too many CISes that share the same high degree node, compared to the baseline of the original Meng et al. method. We used $q = 100$ for both training and validation. The resulting average weighted accuracies of an SPNN trained with the inverse bias w.r.t. the class sizes of relation SH_{100} (eq. (13)) are 0.64 and 0.69 for the baseline and our method, respectively. Note that training considering the classes sizes estimations improves our performance in a scenario where predictions are made per class. We made a paired t-test over the multiple runs resulting in a p-value of 0.03773, which we use to argue that our approach has better performance than the baseline.

C. Evaluating the accuracy of the \hat{F} estimator

#Exp.	Graph	Relation	k	I	#tours	#samples
1	Yeast	PERC	4	100	1k	100k
2	MSR	PERC	4	10k	1k	100k
3	DBLP1	SHs	3	10k	1k	100k

TABLE III: Experiments executed for weight-based motifs counting: datasets, subgraph relations and parameters.

Here, we evaluate the quality of our estimator \hat{F} (eq. (11)), applying MCC (see Sec. IV-A) problem with two subgraph relations: PERC and SH_d (Definitions 5 and 6, respectively) on three datasets (Yeast, DBLP1, and MSR). We focused on the three experiments which is described in Table III. For

Yeast and MSR networks, we consider quasi-cliques with 4 nodes with density greater than 0.5 (i.e., each node must be connected to at least two others), while all 3-node subgraphs are processed in the DBLP1 graph. In all cases, the pattern score estimated by \hat{F} is computed using $g(S) = \frac{1}{C_{R,S}}$.

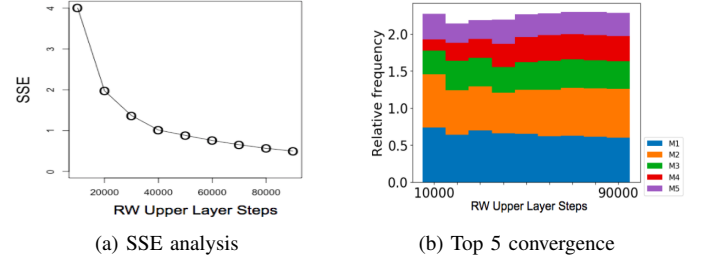


Fig. 2: Exp 1., \hat{F} analysis on Yeast.

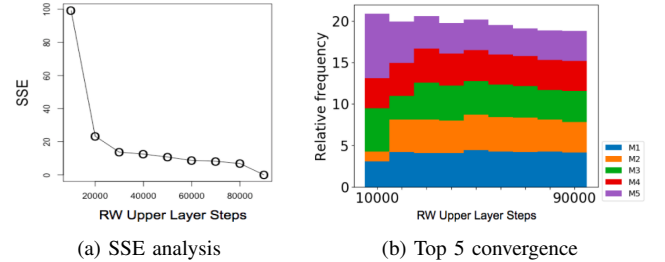


Fig. 3: Exp 2., \hat{F} analysis on MSR.

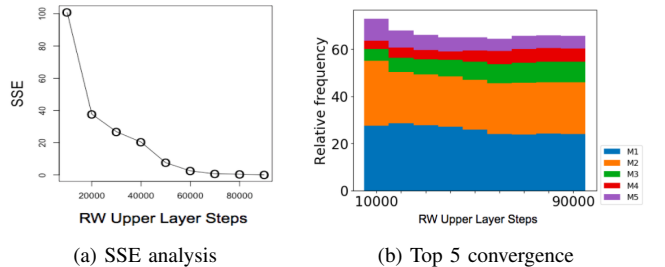


Fig. 4: Exp 3., \hat{F} analysis on DBLP1.

1) *SSE analysis:* First, we will show that our estimator \hat{F} converges to the true value by measuring the sum of squared errors (SSE) of the difference between the estimator and the exact value F (eq. (2)) for all the patterns. The SSE accuracy of **Exp. 1** is shown in Figure 2a). The exact computation of eq. (2) is only possible since the Yeast graph is small. The SSE values go from 4 to 0.5 after 100k sampled subgraphs (Upper Layer steps), showing that our estimator monotonically (and quickly) reduces the estimation error as we sample more subgraphs. Approximate SSE convergences of **Exp. 2** and **Exp. 3** are shown in Figures 3a and 4a, respectively. In these scenarios, we cannot run the exact algorithm due to the

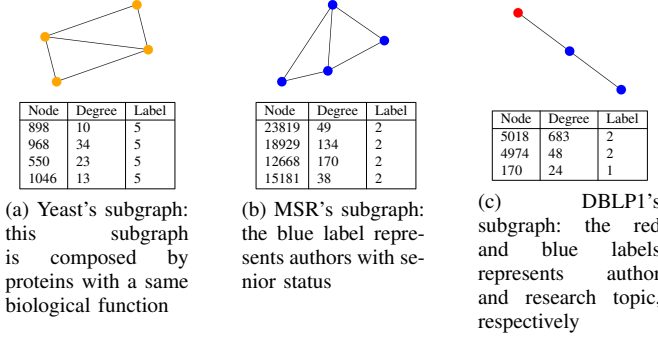


Fig. 5: The patterns and other features of the subgraphs considered in our experiments for $\alpha(R, S)$ estimate analysis.

prohibitive computational cost. Thus, we calculate \hat{F} (eq. (11)) after 100k sampled subgraphs and consider it as ground truth. The goal is to measure convergence. Again, the SSE values reduces in both test scenarios, decreasing from 100 to 0.01 in both, experiments 2 and 3 (Figs. 3a and 4a). This shows that our approach can quickly provide accurate estimates with a relatively few number of subgraph queries.

2) *Top 5 motifs convergence*: Here, we study the fluctuation of estimator \hat{F} for the top 5 motifs of MCC, as we collect more samples (Figs. 2b, 3b and 4b). As we may see, \hat{F} converges as we collect more samples, for all the experiments listed in Table III. This result corroborates with our previous SSE analysis, indicating that the finite-sample bias of our estimator is small.

D. Evaluating the $\hat{\alpha}$ estimator

We now turn our attention to the accuracy of our estimates of $\hat{\alpha}$ from eq. (3) w.r.t. the ground-truth value of α in eq. (1). First, we select three representative CISEs $S \in \mathcal{S}^{(k)}$ shown in Figure 5, one from each experiment in table III. Then, we perform a detailed evaluation of $\hat{\alpha}$ estimator in each of these experimental scenarios. Our main goal is to understand the real-world impact of *supernode* size ($|\mathcal{I}_S|$) and *number of tours* q in the accuracy of $\hat{\alpha}$.

Figure 6 shows the impact of the supernode size in the accuracy of estimating $\alpha(R, S)$ for $g(\cdot) = 1$ (i.e., we are estimating the class's size, $|C_{R,S}|$). The figure shows a boxplot for different supernode sizes and the vertical dotted lines delimit the exact α (eq. (1)). The supernodes were generated using the subgraphs retrieved by the iteration-bounded exact algorithm (Alg. 1) with a budget (described in parentheses). Note that, the budget is generally larger than $|\mathcal{I}_S|$ since the exact algorithm sometimes retrieves subgraphs out of the class of interest. We observe that larger supernode sizes leads to less variance in **Exp. 1** and **Exp. 2**, Figs. 6a and 6b, respectively, specially when the budget to create them was set to 10^5 , where we know more elements of the subgraph classes. On the results for **Exp. 3** (Fig. 6c), the error of estimating α is small because the random walks mix fast, making the tours shorter for all tested supernode sizes.

Theoretically, we know that a larger supernode implies shorter tours in average, as the average tour length is inversely proportional to the total number of edges in the supernode. Thus, the initial cost of having spent more computation in the iteration-bounded exact algorithm leads to a larger supernode, which may pay-off if we can get shorter tours. This behavior is seen in Figure 7, which measures the total number of subgraph queries needed to complete 1000 tours in our estimator $\hat{\alpha}$ accounting for the exact algorithm retrieves budget $B \in \{10^2, 10^3, 10^4, 10^5\}$. The vertical dotted line shows the budget that the exact algorithm required to compute $\alpha(R, S)$ exactly. Note that use a larger budget in the exact algorithm often pays-off in reducing the total number, but of course there is a limit where it start being counter-productive. Also note that our estimators is generally between one and six order of magnitude faster than the exact computation.

We now study the trade-off between $\hat{\alpha}$'s accuracy and the number of tours. Figure 8b shows the estimate of $\alpha(R, S)$ when the supernode is fixed 1k iterations (steps) and the number of tours varies between 10 and 1k. In fact, we may see that the estimate of $\hat{\alpha}$ not only improves when we use more tours, but also it converges to true value (as shown by the boxplots). For practitioners, we advise to test the estimator variance for different number of tours in their specific applications: a diminishing return in variance reduction indicates a good number of tours.

E. Scalability and efficiency

We assess the efficiency and scalability of R-GPM from two perspectives. First, we calculate the cost to compute α for a given class $C_{R,S}$ – in terms of the number of steps – for both the exact DFS method, R-GPM and the best case scenario. The later may be represented by an oracle algorithm which enumerates only the subgraphs that are really necessary ($C_{R,S}$).

Exp.	#Tours	#Steps/Tour	#Steps (Total)	Speedup
Exp. 1	10.00	26.97 \pm 0.93	369.65	481.00x
	100.00	27.30 \pm 0.30	2830.45	62.82x
	1000.00	27.44 \pm 0.09	27536.12	6.46x
	Best #Steps		1073	DFS #Steps 177804
Exp. 2	10.00	832.0 \pm 94.16	9320.08	1971.61x
	100.00	846.92 \pm 30.69	85691.88	214.44x
	1000.00	860.88 \pm 9.61	861880.03	21.32x
	Best #Steps		20572	DFS #Steps 18375595
Exp. 3	10.00	411.46 \pm 2.85	5114.57	71183.73x
	100.00	409.43 \pm 0.89	41942.52	8680.32x
	1000.00	409.48 \pm 0.28	410475.19	886.96x
	Best #Steps		73896	DFS #Steps 364074301

TABLE IV: Comparison between our approach, DFS solution and the best case scenario in terms of the number of steps.

Table IV shows a comparison between the algorithms in **Exp. 2** (with similar results for Exp. 1 and 3). Our approximate solution provides significant computational savings (up to 3 orders-of-magnitude), outperforming the exact method in running time. As expected, the performance gap between these

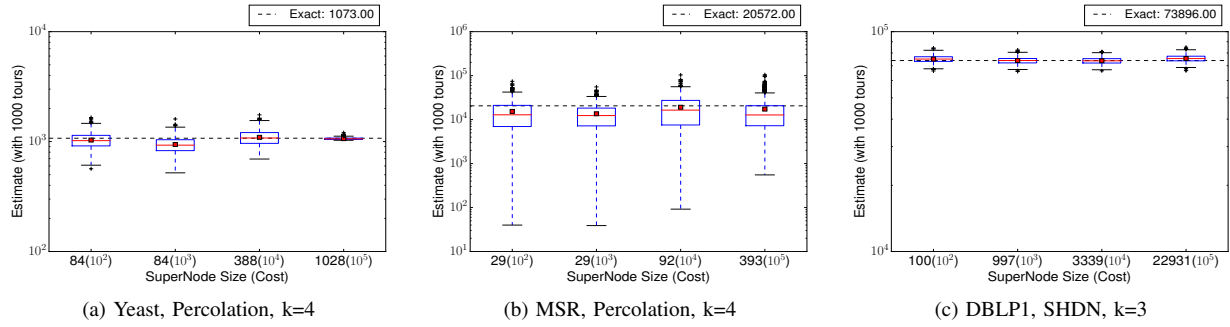


Fig. 6: This figure shows the α_C values returned by our algorithm, varying the supernode size. Increased supernode size reduces variance in Exp. 1 and 2 (Figs. 5a and 5b), but has almost no effect on Exp. 3 (Fig. 5c).

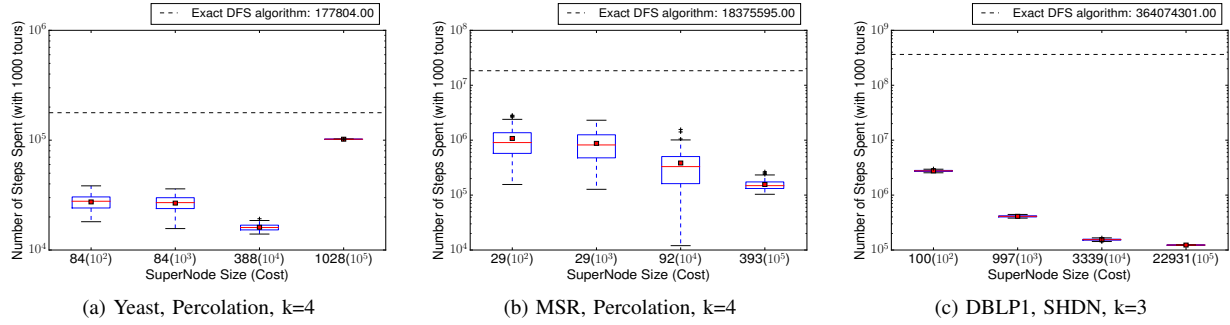


Fig. 7: Total cost (sum of RW steps for 1000 tours + iteration-bounded exact computation) to estimate $\alpha(R, S)$ for different supernode sizes. Larger supernodes boost the efficiency of our method since much less steps are performed in the RW tour. The dashed line shows the effort needed to compute the exact BFS-based algorithm.

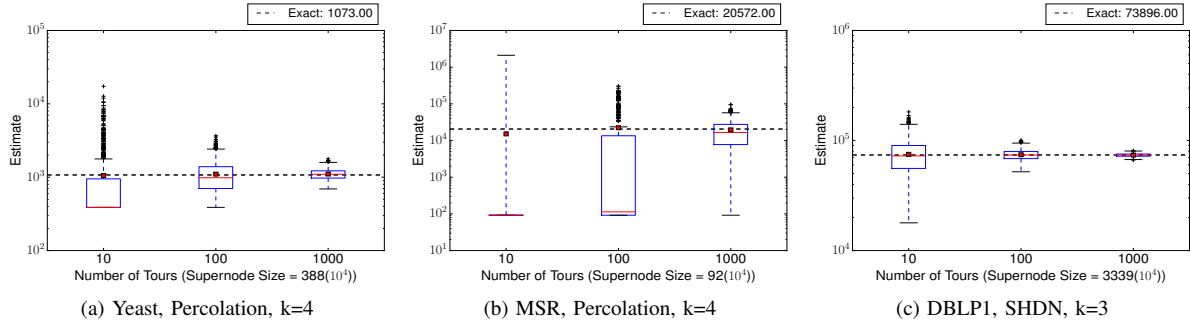


Fig. 8: Accuracy evaluation of α_C , varying the number of tours performed. The budget to build the supernode set was fixed to 1k iterations (steps). As expected, the variance reduces as the supernode size increases, improving the quality of the estimator.

algorithms decreases as we increase the number of tours used to estimate $\alpha(R, S)$. There is an “accuracy vs. efficiency” trade-off, since the estimate gets more accurate as we increase the number of tours or supernode size.

Table V shows the execution time and respective speedups of R-GPM on the three datasets. In all of them, we compute in parallel the statistics for 10k subgraphs (i.e., the number of subgraphs sampled in the upper lower RW). The remaining configurations are the same used in the previous experiments (Table III). As we may realize, R-GPM provides a near-

linear speedup in all of our tests, showing the benefits of our parallelization strategy. The super-linear behaviour of R-GPM in the Yeast graph is explained by the graph being small enough to fit in the memory cache.

V. RELATED WORK

Existing methods for estimating induced subgraph statistics of graphs are focused on simple subgraph counting tasks. For instance, edge-based algorithms sample edges and combine them to estimate subgraphs counts [34] and triangles [35].

Dataset	#cores			Speedup
	11	22	44	
Yeast	5m6s	2m36s	1m27s	x3.5
MSR	338m49s	176m32s	125m54s	x2.7
DBLP1	1002m16s	522m26s	322m19s	x3.1

TABLE V: R-GPM’s running time analysis

There are drawbacks to these methods: (a) the inability to consider larger subgraphs, (b) the cost to remove the bias of sampling a particular edge and, (c) the need of having access to the entire network. Methods based on random walks were proposed to address these challenges.

There are RW solutions focused on estimating simple graph statistics [25], [36]. In a complementary direction, Hasan and Zaki [17] proposed a MCMC algorithm that works on chain of subgraph patterns from a input graph, where their goal was sample a subset of interesting patterns uniformly. Wang et al. [18] and Bhuiyan et al. [19] develop two sampling methods to deal with motifs and graphlet counting, using RWs and high-order networks. Such solutions differ in the way they remove the bias from sampling: one uses Horvitz-Thompson estimator and the second employs a Metropolis-Hastings algorithm.

Recently, MCMC methods sample subgraphs by walking in the actual graph structure rather than high-order networks [37]. For that, they keep not only the the most recent visit node, but the last k nodes visited by the RW. Subgraphs are derived from these nodes and the bias of sampling them are computed according pre-established equations. Although walking in the original graph may be faster than to perform MCMC in a high-order network, these methods are not amenable to the subgraph relationships and classes introduced in our work.

VI. CONCLUSIONS

This paper introduces the concept of subgraph relations and its applications to graph pattern mining and learning problems. Relations generalize traditional GPM problems and they can aid the analysis of subgraph patterns. In particular, we saw that (1) subgraph relations can help reduce learning biases associated with locally subgraph-dense regions (e.g., high-degree nodes) and (2) subgraph classes may provide novel and interesting analysis on motifs in graphs. Finally, we show that our proposed hybrid exact-sampling estimator is consistent, accurate and significantly faster than the exact approach alone.

Acknowledgements. This work was partially supported by CNPq, CAPES, Fapemig, INCT-Cyber, MasWeb, EuBra-BigSea, Atmosphere and by the ARO, under the U.S. Army Research Laboratory award W911NF-09-2-0053. Any opinions, findings and conclusions or recommendations expressed in this material are those of the authors and do not necessarily reflect the views of ARO.

REFERENCES

[1] M. Kuramochi and G. Karypis, “Finding frequent patterns in a large sparse graph,” *Data mining and knowledge discovery*, 2005.

[2] G. Preti, M. Lissandrini, D. Mottin, and Y. Velegrakis, “Beyond frequencies: Graph pattern mining in multi-weighted graphs,” in *Edbt*, vol. 18, 2018, pp. 169–180.

[3] C. Jiang, F. Coenen, and M. Zito, “A survey of frequent subgraph mining algorithms,” *The Knowledge Engineering Review*, 2013.

[4] A. Buzmakov, S. O. Kuznetsov, and A. Napoli, “Efficient mining of subsample-stable graph patterns,” in *ICDM*, 2017.

[5] C. Meng, S. C. Mouli, B. Ribeiro, and J. Neville, “Subgraph pattern neural networks for high-order graph evolution prediction,” in *AAAI*, 2018.

[6] R. Milo, S. Shen-Orr, S. Itzkovitz, N. Kashtan, D. Chklovskii, and U. Alon, “Network motifs: simple building blocks of complex networks,” *Science*, 2002.

[7] H. Choi, J. Son, Y. Cho, M. K. Sung, and Y. D. Chung, “Spider: A system for scalable, parallel / distributed evaluation of large-scale rdf data,” in *CIKM*, 2009.

[8] I. Derényi, G. Palla, and T. Vicsek, “Clique percolation in random networks,” *Physical Review Letters*, 2005.

[9] A. R. Benson, D. F. Gleich, and J. Leskovec, “Higher-order organization of complex networks,” *Science*, 2016.

[10] K. Shin, T. Eliassi-Rad, and C. Faloutsos, “Corescope: Graph mining using k-core analysis-patterns, anomalies and algorithms,” in *ICDM*, 2016.

[11] D. Koutra, U. Kang, J. Vreeken, and C. Faloutsos, “Summarizing and understanding large graphs,” *Statistical Analysis and Data Mining: The ASA Data Science Journal*, 2015.

[12] H. Robbins and S. Monro, “A stochastic approximation method,” *The annals of mathematical statistics*, 1951.

[13] G. Palla, I. Derényi, I. Farkas, and T. Vicsek, “Uncovering the overlapping community structure of complex networks in nature and society,” *Nature*, 2005.

[14] T. Junttila and P. Kaski, “Engineering an efficient canonical labeling tool for large and sparse graphs,” in *2007 Proceedings of the Ninth Workshop on Algorithm Engineering and Experiments (ALENEX)*. SIAM, 2007, pp. 135–149.

[15] M. Kuramochi and G. Karypis, “Frequent subgraph discovery,” in *ICDM*, 2001.

[16] J. Huan, W. Wang, and J. Prins, “Efficient mining of frequent subgraphs in the presence of isomorphism,” in *ICDM*, 2003.

[17] M. Al Hasan and M. J. Zaki, “Output space sampling for graph patterns,” *Proc. VLDB Endow.*, 2009.

[18] P. Wang, J. C. S. Lui, B. Ribeiro, D. Towsley, J. Zhao, and X. Guan, “Efficiently estimating motif statistics of large networks,” *TKDD*, 2014.

[19] M. Rahman, M. A. Bhuiyan, M. Rahman, and M. A. Hasan, “GUISE: a uniform sampler for constructing frequency histogram of graphlets,” *Knowl. Inf. Syst.*, 2014.

[20] C. Cooper, T. Radzik, and Y. Siantos, “Fast low-cost estimation of network properties using random walks,” *Internet Mathematics*, 2016.

[21] K. Avrachenkov, B. Ribeiro, and J. K. Sreedharan, “Inference in osns via lightweight partial crawls,” *SIGMETRICS*, 2016.

[22] N. Alon, I. Benjamini, E. Lubetzky, and S. Sodin, “Non-backtracking random walks mix faster,” *Communications in Contemporary Mathematics*, 2007.

[23] C.-H. Lee, X. Xu, and D. Y. Eun, “Beyond random walk and metropolis-hastings samplers: why you should not backtrack for unbiased graph sampling,” in *ACM SIGMETRICS Performance evaluation review*, 2012.

[24] L. Lovász, “Random walks on graphs: A survey,” in *Combinatorics, Paul Erdős is Eighty*, 1996.

[25] B. Ribeiro and D. Towsley, “Estimating and sampling graphs with multidimensional random walks,” in *IMC*, 2010.

[26] —, “On the estimation accuracy of degree distributions from graph sampling,” in *CDC*, 2012.

[27] C. A. Stewart, T. M. Cockerill, I. Foster, D. Hancock, N. Merchant, E. Skidmore, D. Stanzione, J. Taylor, S. Tuecke, G. Turner *et al.*, “Jetstream: a self-provisioned, scalable science and engineering cloud environment,” in *Proceedings of the 2015 XSEDE Conference: Scientific Advancements Enabled by Enhanced Cyberinfrastructure*, 2015, pp. 1–8.

[28] D. Bu, Y. Zhao, L. Cai, H. Xue, X. Zhu, H. Lu, J. Zhang, S. Sun, L. Ling, N. Zhang *et al.*, “Topological structure analysis of the protein-protein interaction network in budding yeast,” *Nucleic acids research*, 2003.

[29] Y. Sun, R. Barber, M. Gupta, C. C. Aggarwal, and J. Han, “Co-author relationship prediction in heterogeneous bibliographic networks,” in *ASONAM*, 2011.

- [30] J. Tang, J. Zhang, L. Yao, J. Li, L. Zhang, and Z. Su, "Arnetminer: extraction and mining of academic social networks," in *KDD*, 2008.
- [31] N. Pržulj, "Biological network comparison using graphlet degree distribution," *Bioinformatics*, 2007.
- [32] G. Liu and L. Wong, "Effective pruning techniques for mining quasi-cliques," in *ECML-PKDD*, 2008.
- [33] B. Delyon, "General results on the convergence of stochastic algorithms," *IEEE Transactions on Automatic Control*, 1996.
- [34] N. K. Ahmed, N. Duffield, J. Neville, and R. Kompella, "Graph sample and hold: A framework for big-graph analytics," in *KDD*, 2014.
- [35] M. Jha, C. Seshadhri, and A. Pinar, "A space efficient streaming algorithm for triangle counting using the birthday paradox," in *KDD*, 2013.
- [36] S. J. Hardiman and L. Katzir, "Estimating clustering coefficients and size of social networks via random walk," in *WWW*, 2013.
- [37] G. Han and H. Sethu, "Waddling random walk: Fast and accurate mining of motif statistics in large graphs," in *ICDM*, 2016.